[8] S. Nojima, "Enhancement of optical gain in two-dimensional photonic crystals with active lattice points," *Jpn. J. Appl. Phys.*, vol. 37, no. 2, pp. L565–L567, 1998.
[9] J. P. Dowling, M. Scalora, M. J. Bloemer, and C. M. Bowden, "The photonic band edge laser: A new approach to gain enhancement," *J. Appl. Phys.*, vol. 75, pp. 1896–1899, 1994.
[10] K. Sakoda, "Enhanced light amplification due to group-velocity anomaly peculiar to two- and three-dimensional photonic crystals," *Opt. Express*, vol. 4, pp. 167–176, 1999.
[11] M. Sasada, A. Yamanaka, K. Sakoda, K. Inoue, and J. W. Haus, "Laser oscillation from dye molecules in a 2-D photonic crystal," in *Tech. Dig. Pacific Rim Conf. Lasers and Electro-Optics*, 1997, pp. 42–43.
[12] M. Imada, S. Noda, A. Chutinan, and Y. Ikenaga, "Light-emitting devices with one- and two-dimensional air/semiconductor gratings embedded by wafer fusion technique," in *Dig. IEEE Int. Semiconductor Laser Conf.*, 1988, pp. 211–212.
[13] K. Inoue, M. Sasada, J. Kawamata, K. Sakoda, and J. W. Haus, "A two-dimensional photonic crystal laser," *Jpn. J. Appl. Phys.*, vol. 38, pp. L157–L159, 1999.
[14] K. Ohtaka, "Energy band of photon and low-energy photon diffraction," *Phys. Rev. B*, vol. 19, pp. 5057–5067, 1979.
[15] K. Ohtaka and Y. Tanabe, "Photonic bands using vector spherical waves—I: Various properties of Bloch electric fields and heavy photons," *J. Phys. Soc. Jpn.*, vol. 65, pp. 2265–2275, 1996.
[16] ———, "Photonic bands using vector spherical waves—II: Reflectivity, coherence and local field," *J. Phys. Soc. Jpn.*, vol. 65, pp. 2276–2284, 1996.
[17] K. Ohtaka, T. Ueta, and K. Amemiya, "Calculation of photonic bands using vector cylindrical waves and reflectivity of light for an array of dielectric rods," *Phys. Rev. B*, vol. 57, pp. 2550–2568, 1998.
[18] J. M. Ziman, *Theory of Solids.* Cambridge: Cambridge Univ. Press, 1977, p. 146.
[19] J. A. Stratton, *Electromagnetic Theory.* New York: McGraw-Hill, 1941, p. 397.
[20] K. L. Kliewer and R. Fuchs, "Optical modes of vibration in an ionic crystal slab including retardation—II: Radiative region," *Phys. Rev.* vol. 150, pp. 573–588, 1966.
[21] R. Fuchs, K. L. Kliewer, and W. J. Pardee, "Optical properties of an ionic crystal slab," *Phys. Rev.*, vol. 150, pp. 589–596, 1966.
[22] K. Ohtaka, Y. Suda, S. Nagano, T. Ueta, A. Imada, T. Koda, J. S. Bae, K. Mizuno, S. Yano, and Y. Segawa, submitted for publication.
[23] K. Ohtaka and S. Yamaguchi, unpublished.
[24] A. Yariv, *Quantum Optics*, 3rd ed. New York: Wiley, 1989, p. 407.
[25] H. C. Casey, Jr. and M. B. Panish, *Heterostructure Lasers: Part A, Fundamental Principles.* New York: Academic, 1978, section 2.10.
[26] K. Ohtaka, T. Ueta, and K. Sakoda, submitted for publication.
[27] K. Sakoda, K. Ohtaka, and T. Ueta, "Low-threshold laser oscillation due to group-velocity anomaly peculiar to two- and three-dimensional photonic crystals," *Opt. Express*, vol. 4, no. 12, pp. 481–489, 1999.
[28] E. Yablonovitch, "Inhibited spontaneous emission in solid-state physics and electronics," *Phys. Rev. Lett.*, vol. 58, pp. 2059–2062, 1987.

Kazuo Ohtaka received the Bachelor, Master, and Ph.D. degrees in engineering from the Department of Applied Physics, University of Tokyo, Tokyo, Japan, in 1965, 1967, and 1970, respectively.

He joined the theoretical solid state group of the same department in 1969 and shifted to Chiba University in 1989, where he is currently a Professor at the Center for Frontier Science, Chiba University, Japan. He has been working in the field of theoretical solid-state physics. In a previous work, he successfully formulated the band structure calculation for a periodic array of dielectric spheres. He and his collaborators wrote several papers then, concerning light scattering in a periodic system of spheres. In 1983, his interest shifted to the field of the Fermi-edge effect of electrons in simple metals, and in 1996, he returned to the field of photonic crystals.

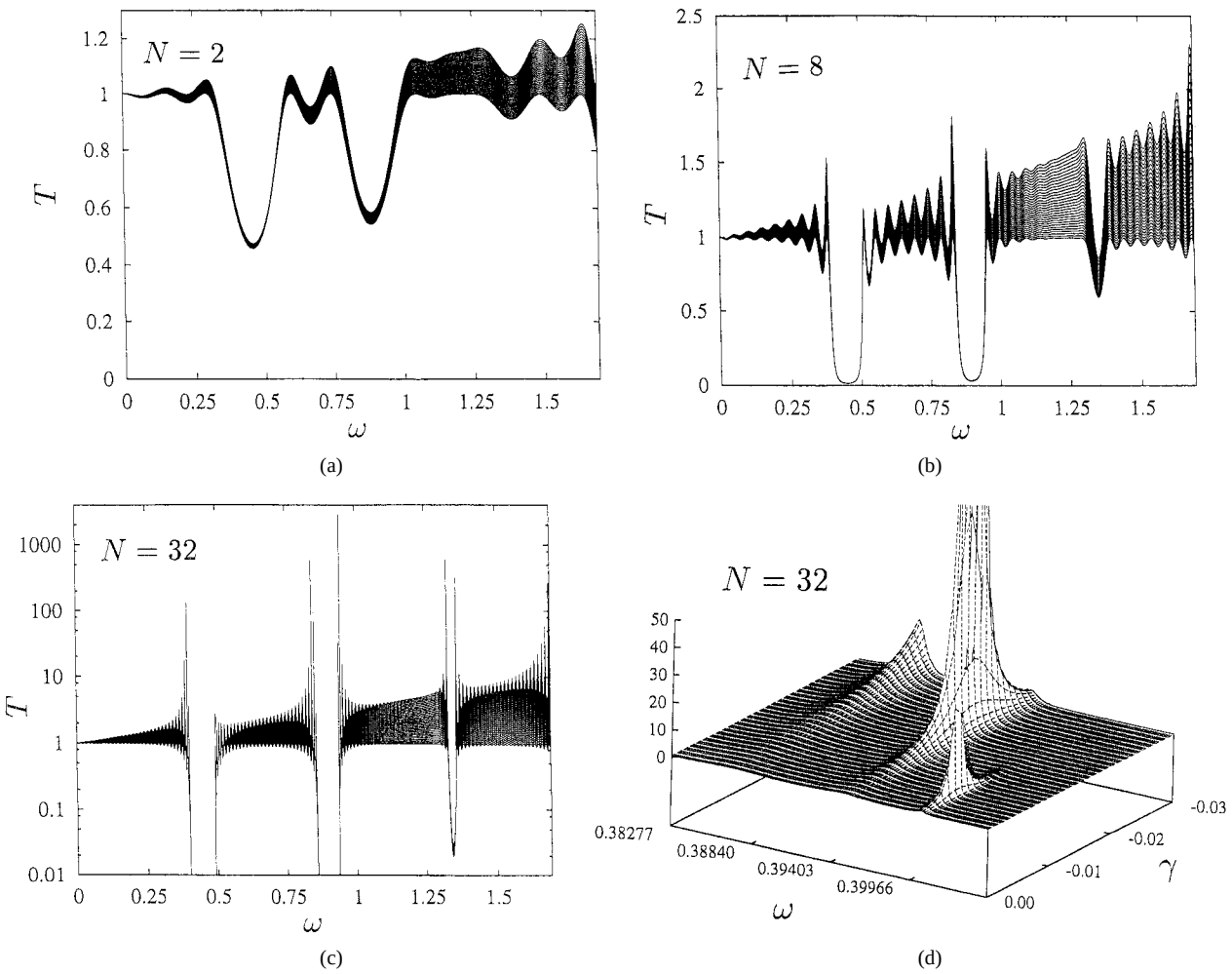

Fig. 8. Front view of the transmittivity of light for an active 1-D photonic crystal. The transmittivity for $0 < \omega < 1.7$ is shown. The height of the T surface along a fixed value of γ is shown versus ω. The range of γ taken into account is $0 > \gamma > -0.03$, as in Figs. 6 and 7, with the spacing 0.001 of the selected values of γ. The thickness of the stacked films is: (a) $N = 2$, (b) $N = 8$, and (c) $N = 32$. Note the scale change of the vertical axis in the case of $N = 32$. The panel (d) shows a bird's-eye view of the T surface of $N = 32$ near the lower edge of the first bandgap.

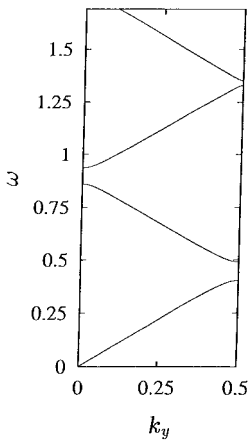

Fig. 9. Band structure of a regular array of thin films. The wave vector is $\boldsymbol{k} = (0, k_y, 0)$, k_y being the component in the thickness direction.

of lasing in photonic crystals and compare it with a multilayer stack of thin films.

It is shown that a photonic band of 1-D systems has nearly the same lasing properties irrespective of the band position in frequency. This is in clear contrast to the lasing in 2-D or 3-D photonic crystals, in which the onset of the lasing in a higher band is much easier than in the first band. The discussion for these results has been given in terms of the band structure and the Q values of the slab modes.

ACKNOWLEDGMENT

The author acknowledges the collaboration of his colleagues Prof. K. Sakoda and Dr. T. Ueta.

REFERENCES

[1] J. D. Joannopoulos, R. D. Meade, and J. N. Winn, *Photonic Crystals.* Princeton, NJ: Princeton Univ. Press, 1995.
[2] C. M. Soukoulis, Ed., *Photonic Band Gaps and Localization.* New York: Plenum, 1993.
[3] ———, *Photonic Band Gap Materials.* Dordrecht: Kluwer, 1996.
[4] J. P. Dowling and C. M. Bowden, "Atomic emission rates in inhomogeneous media with application to photonic band," *Phys. Rev. A,* vol. 46, pp. 612-625, 1992.
[5] ———, "Beat radiation from dipoles near a photonic band edge," *J. Opt. Soc. Amer. B,* vol. 10, pp. 353–363, 1993.
[6] S. John and T. Quang, "Spontaneous emission near the edge of a photonic band gap," *Phys. Rev. A,* vol. 50, pp. 1764–1769, 1994.
[7] T. Suzuki and P. K. L. Yu, "Emission power of an electric dipole in the photonic band structure of the FCC lattice," *J. Opt. Soc. Amer. B,* vol. 12, pp. 570–582, 1995.

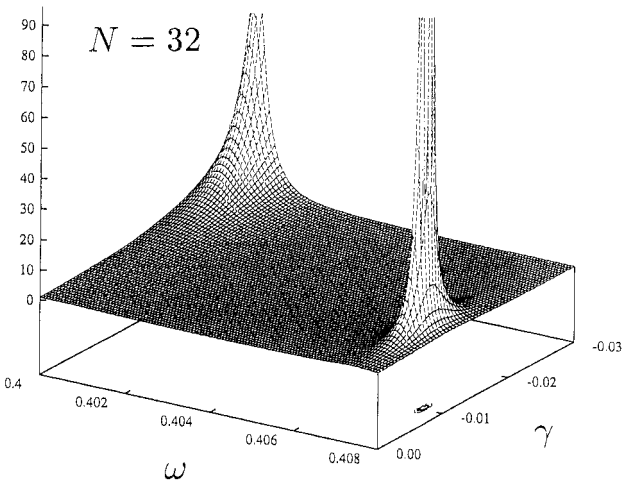

Fig. 6. T surface in a narrow region near the lower edge of the bandgap. The case of $N = 32$ is the first case in the layer-doubling process that has a peak on the T surface within the calculated range of $\gamma > -0.03$. Only the region of active cylinders, i.e., the region of $\gamma < 0$, is shown.

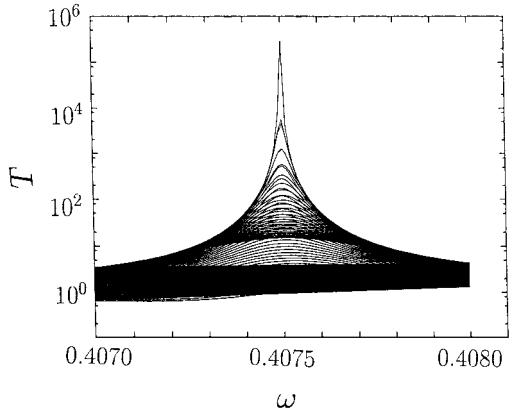

Fig. 7. Front view of the peak of Fig. 6. A very small range of ω in the immediate vicinity of the band edge is shown. The peak height is over 10^5.

surface starts to occur along a ridge, and when $N = 32$, we have a divergent peak just at a frequency in the vicinity of the upper boundary of the bandgap.

It is interesting to compare the present result with that of multilayer stacks of thin films, a typical 1-D photonic crystal. Since 1-D systems are much easier to prepare than a periodic array of cylinders, the latter must be beneficial enough for the efforts of its fabrication to be justified.

Fig. 8 is related with the T surface for a periodic repetition of parallel thin films. The active thin films are assumed to have the same dielectric constant as (7), and its thickness is put to 0.28, so that the volume fraction will be the same as that examined above (the radius of $a = 0.3$ of the cylinders in a square lattice gives the volume fraction of 0.28). The frequency ω used in the figure is normalized by the periodicity of the multilayer as before. In this calculation, we checked that a conspicuous enhancement of the T surface happens only for $N \geq 16$, within the calculated range of $|\gamma| < 0.03$. The result we are showing is for $N = 32$. We show the front view of the T surface over the wider frequency range of $0 < \omega < 1.7$.

The result is rather discouraging; we must admit that, as far as the first bandgap is concerned, the onset of the lasing in the 1-D system and the array of cylinders is not very different. This stems from the fact that the first bandgap of the array of cylinders occurs mainly from the folding effect involving the shortest reciprocal lattice vector (0, 1, 0) (as for the bandgap at $k_y = 0.5$); it is mainly of 1-D nature in spite of the 2-D character in geometry.

Another point to be noted in Fig. 8 is that in a 1-D photonic crystal, no essential features are observed that characterize the lasing involving the bandgaps in a higher frequency range. This is a general characteristic of 1-D systems, not limited to the one examined here, as is easily understood in terms of the band structure of the 1-D photonic crystal shown in Fig. 9; even a band in a higher frequency range has similar bandwidth and curvature to the first band. This is in clear contrast to the case of 2-D or 3-D photonic crystals, which have bands of very flat dispersion in a higher frequency region. In fact, our previous paper demonstrated several striking characteristics occurring near the higher bandgaps of a 2-D photonic crystal [26], [27]: very low values of N (sometimes, even $N = 1$) needed for the laser action, a drastically reduced threshold value of γ (sometimes, $|\gamma_{\rm th}|$ on the order of 0.001 or less, i.e., less than one-tenth, sometimes one-hundredth, of the value seen above), and a simultaneous appearance of several lasing peaks. The efforts of fabrication will thus pay well only if we make use of the lasing on higher photonic bands.

It is important, however, to note that we have not taken into account in the present work the lifetime of an atom. In case the radiative decay is a main origin of the atomic lifetime, a system of 2-D or 3-D photonic crystal works much more positively than the 1-D ones in enhancing the Q value of the *atomic* levels. We can estimate the threshold value of the population inversion from the calculated values of $\gamma_{\rm th}$ if we express γ of the dielectric constant in a Lorentzian form with a width determined by the spontaneous radiative decay. In such a treatment, the advantageous features of 2-D or 3-D photonic crystals over the 1-D ones will be explicit even for the first bandgap. This will be a main benefit of photonic crystals, claimed widely in the literature [28].

V. Summary

We have given a method of calculating the density of states of electromagnetic normal modes of a slab photonic crystal. Using it, we have shown that the Q values of the standing-wave modes of the slab increase as the thickness increases.

To understand the role of the Q values of slab modes in the laser oscillation, we calculated the transmittivity of light for an active photonic crystal of arrayed cylinders. We assigned to the cylinders a complex dielectric constant with an imaginary part γ, which is taken to be negative to describe the amplification of light in the active photonic crystal. It is found that the transmittivity of light has divergent peaks, indicative of the onset of the laser oscillation, in the parameter space of (ω, γ, N), N being the number of the 2-D layers in the thickness direction. From the peak position in the parameter space, we obtained the threshold value γ required for the onset

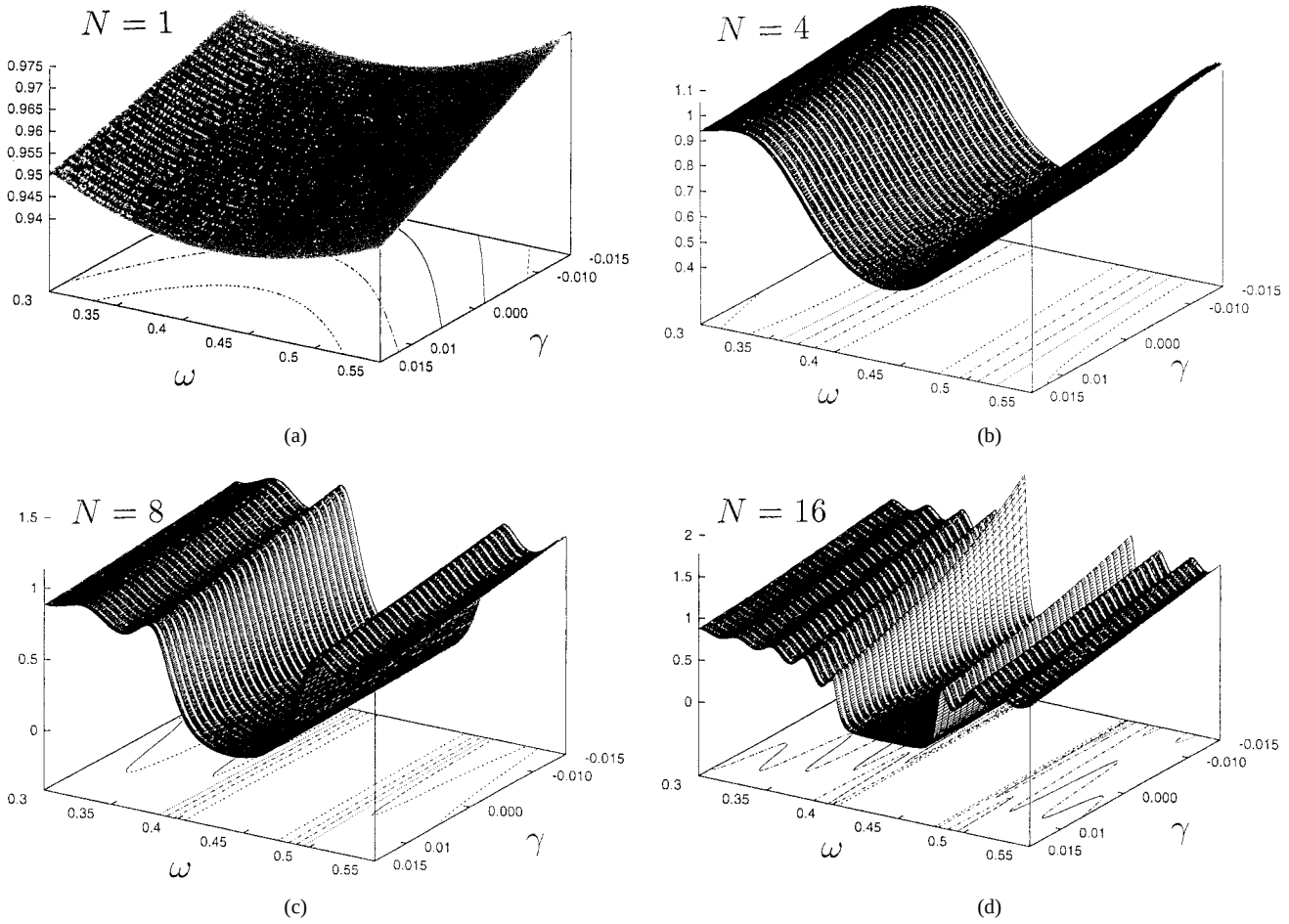

Fig. 5. Transmittivity of z-polarized light as a function of ω and γ for a slab of arrayed cylinders. The region of $\gamma > 0$ corresponds to the lossy dielectric cylinders, and that of $\gamma < 0$ represents the active cylinders. The region of $0.015 > \gamma > -0.015$ is calculated. The thickness of the slab is $N = 1$ in (a), $N = 4$ in (b), $N = 8$ in (c), and $N = 16$ in (d).

in the z direction. The first bandgap is located in the range $0.408 < \omega < 0.42$. Now we calculate the transmittivity of an incident light to see the effect of the negative γ. We used a light of normal incidence and polarized in the z direction. We plot the transmittivity T as a function of (ω, γ). By sweeping (ω, γ) and plotting T in the vertical direction, we may obtain a surface of transmittivity in the three-dimensional (3-D) space, which we call in what follows the T surface. We sweep the range $0.015 > \gamma > -0.03$ to look for a divergent peak on the T surface. When N is small and the Q values of the slab modes are small, it will be difficult to find a divergence in the calculated region of (ω, γ). First, let us see what happens in the frequency range in the neighborhood of the first bandgap.

Fig. 5 shows the N dependence of the T surface in the region of $0.3 < \omega < 0.55$ and $0.015 > \gamma > -0.015$. The two branches of bands, drawn by the solid curves in Fig. 4, are thus excited (in the case of a thick slab). The region of positive γ corresponds to the lossy dielectric cylinders, and the one of negative γ describes the gain of active cylinders. We see that, as N increases, the T surface gradually reflects the band structure, i.e., the stop band corresponding to the first bandgap becomes gradually recognizable. For the cases of $N = 1, 2, 4$, the height of the T surface increases linearly with $|\gamma|$ in the calculated range of γ. The number of interference fringes increases with N. At $N = 8, 16$, we observe a conspicuous increase of the T surface on the edges of the first bandgap. Especially, the T surface of $N = 16$ increases nonlinearly with increasing $|\gamma|$.

Fig. 6 shows the magnified plot of the case of $N = 32$. We examine the lower edge of the bandgap, restricting ourselves to a very small ω range of $0.40 < \omega < 0.41$ and to an active region of $0 > \gamma > -0.03$. Note that we are sweeping a wider range of active γ twice as large as Fig. 5. We find at last a peak on the T surface at $\omega \sim 0.407$ and $\gamma \sim 0.01$. It shows the onset of lasing, if the peak is in fact divergent. The value of $|\gamma|$ of the position of the peak then gives the threshold value $\gamma_{\rm th}$ for the laser action. From the position of the peak we find $|\gamma_{\rm th}| = \sim 0.01$.

That the peak in Fig. 6 is indeed divergent is seen in Fig. 7, which shows the front view of the peak in a logarithmic scale. Each solid curve shows the height of the T surface along a line of a fixed value of γ. We find that the height of the peak is over 10^5. With finer steps of the calculated ω and γ, the peak would be divergent.

We have so far examined the frequency range of the lower side of the bandgap. On the upper side of the bandgap, we have confirmed that nearly the same feature happens in the N dependence: when $N = 16$, the nonlinear growing of the T

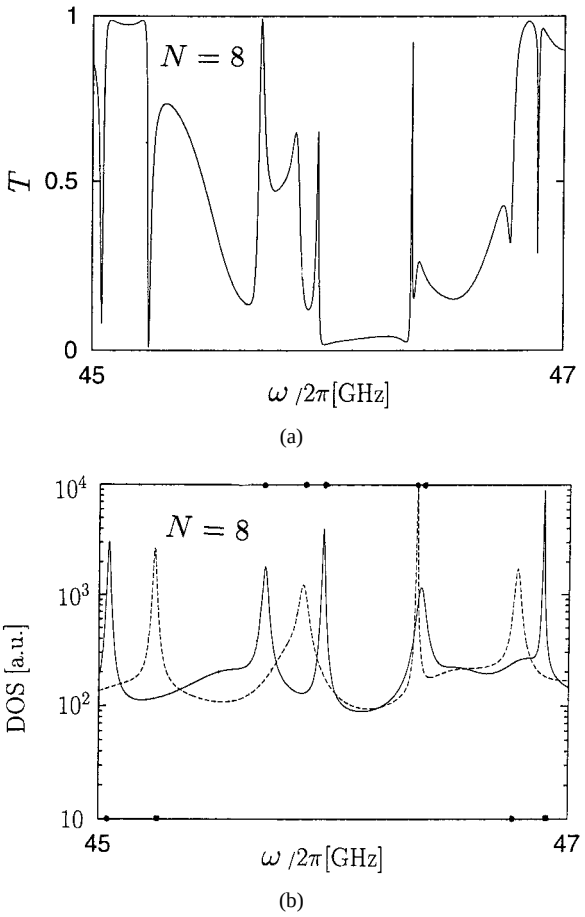

Fig. 3. Correspondence of the fine structures of the transmittivity of light and the DOS of the EM normal modes. The result of the case of $N = 8$ is shown. The transmittivity in (a) is calculated for an S-polarized incident light with the lateral components of the incident wave-vector of $k_x = 0.1$ and $k_z = 0.2$. The DOS in (b) is calculated for the modes of the same wave-vector components. The positions of the sharp peaks (dips) of the transmittivity are marked on the upper (lower) horizontal axis of the panel (b), to confirm the agreement of the positions of the fine structures between the two panels.

narrowing much more pronounced than the average, estimated from the total bandwidth and number of interference fringes.

Fig. 3 shows the ω dependences of the transmittivity (a) in DOS and (b) for the case of $N = 8$. Since the stop band corresponding to the bandgap in Fig. 1(b) is almost complete, it is concluded that the thickness larger than $N \geq 8$, roughly $N \geq 10$, is necessary for the bandgap of $N = \infty$ to be realized in a slab.

As for the correspondence between Fig. 3(a) and (b), we see a precise agreement between the DOS peaks and positions of the fine structures of the transmittivity. However, note that the peaks of the transmittivity marked on the upper horizontal axis and the dips marked in the lower axis both coincide very well with the peak positions of DOS. The conclusion is thus that a DOS peak can lead sometimes to a dip and other times to a peak in transmittivity. This remark is more valid than the one made in our previous study [22], where the DOS peaks were concluded to induce the dips in transmittivity. The variety results from the existence of a series of complex poles in the complex frequency plane; a peak or dip appears in the transmission amplitude depending on the relative phase between the residues of the pole under consideration and

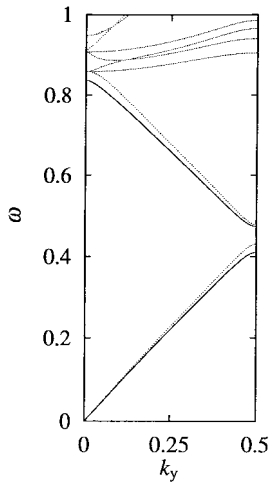

Fig. 4. Band structure of a square array of cylinders for $\boldsymbol{k} = (0, k_y, 0)$. See the text for the parameters of the cylinders. The electric fields of the two bands shown by the bold curves are z polarized. The onset of the laser oscillation near the bandgap between them is examined for a z-polarized light in Fig. 5.

those of the nearby poles. Note also that the line shapes of DOS and transmittivity are not always sinusoidal. If it were sinusoidal, the rule of thumb would yield a right order of magnitudes of the lifetime of a standing-wave mode in a slab. The observed feature implies that a precise quantitative estimation of the lifetime is impossible without a detailed calculation. Nevertheless, the qualitative validity of the rule of thumb is still important. For example, a smaller dispersion of a band is attributed to a smaller energy leakage of a original WGM and has generally a longer lifetime in a slab.

IV. Onset of Lasing in a Photonic Band

The way of looking for the divergence of a transport coefficient is often applied to examine a critical value of a phase transition, the transition temperature of superconductivity, for example. In the optoelectronics, the onset of the lasing in distributed feedback (dfb) lasers was first examined by this method by Yariv [24], who used as a test transport coefficient the transmittivity of an active semiconductor system with one-dimensional (1-D) periodic grooves on its surface. The way adopted here is not other than his method. Conceptually, the lasing in a photonic crystal indeed belongs to the same category as the dfb lasers [25].

The system we analyze in this section is the periodic array of cylinders of active substance. The population inversion is incorporated into the negative imaginary part γ of the dielectric constant ε of the cylinders. We assume

$$\varepsilon = 2.0 + i\gamma \tag{7}$$

with the real part put to 2.0 throughout the paper. The cylinders are arrayed in the square lattice of lattice constant d. The radius a of the cylinders, normalized by d, is taken to be 0.3, and the frequency ω of light, normalized by $2\pi/d$, is swept in the frequency range $0 < \omega < 1.0$. We take the xz plane parallel to the plane of the layer with the z axis chosen in the cylinder axis. The y direction is thus the thickness direction.

We show in Fig. 4 the band structure for the wave vector $(0, k_y, 0)$ of the infinite crystal, dropping γ in (7). The bold curves show two bands with the polarization of electric field

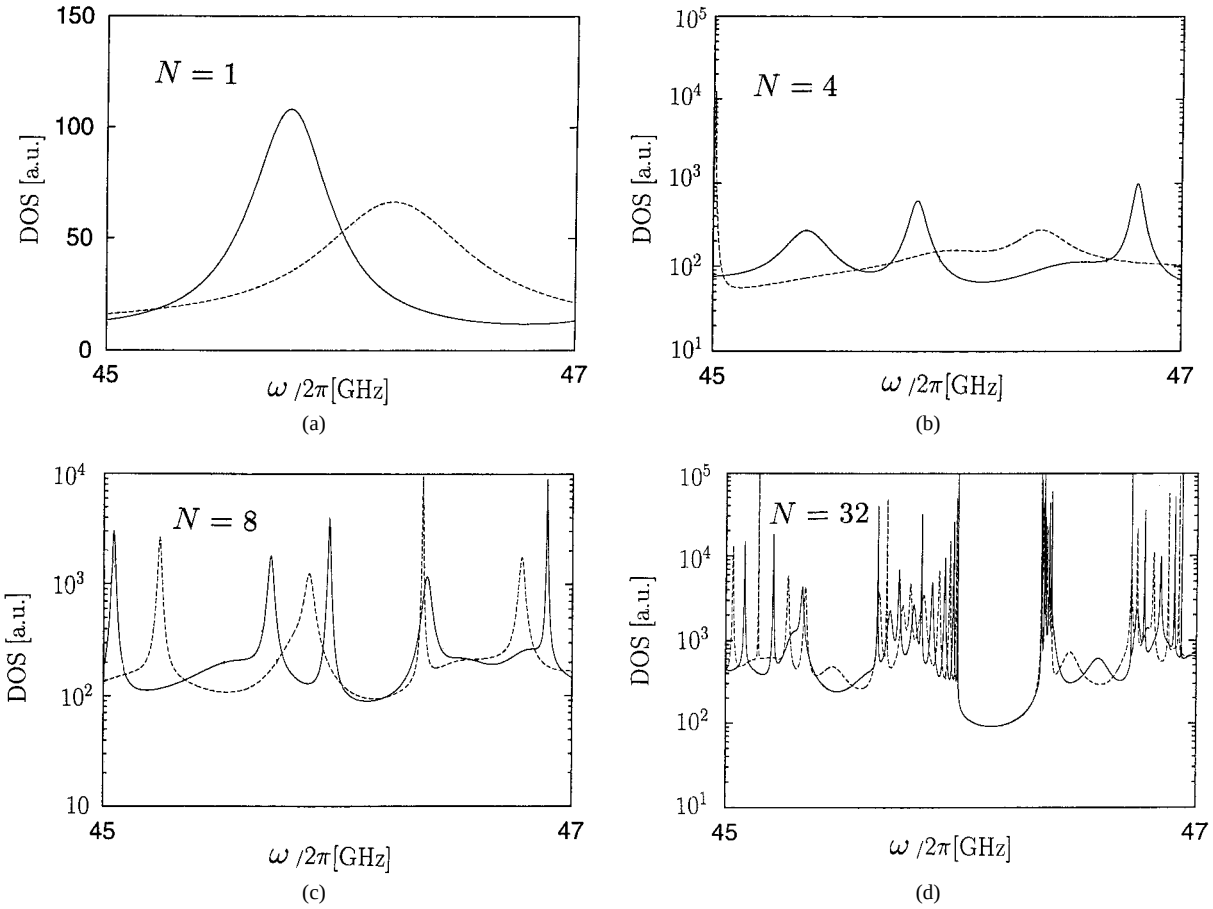

Fig. 2. Increment per sphere of the DOS of the EM modes with $k_x = 0.1$ and $k_z = 0.2$: (a) for $N = 1$, (b) for $N = 4$, (c) for $N = 8$, and (d) for $N = 32$. The DOS of even-parity modes is drawn by solid curves and of odd-parity modes by dashed curves.

of diffraction in the normal incidence. The vector KKR equation includes $l \leq 6$ to obtain Fig. 1. Of course the result corresponds to the case of $N = \infty$, i.e., to an infinite photonic crystal. There are many bands occurring from the degeneracy of WGM of a sphere and from the folding effects associated with 2-D reciprocal lattice vectors. Fig. 1(b) shows the magnified plot for the narrow frequency range of $0.48 < \omega < 0.50$, which corresponds to 45 GHz $< \omega/2\pi <$ 47 GHz. The overall band structure is not straightforward. We can recognize an effect of band crossing. Note the presence of a bandgap bounded by a very flat band from above.

The increment of DOS for the frequency range of 45 GHz $< \omega/2\pi <$ 47 GHz is shown in Fig. 2 for a slab photonic crystal. To grasp a rough image of the DOS of slab modes, we can imagine that k_y is quantized in Fig. 1. In Fig. 2(a)–(d), we show DOS for the slab of $N = 1, 4, 8, 32$, respectively. Fig. 2(d) for $N = 32$ reflects the band structure faithfully; of the three large valleys, the central one corresponds to the bandgap and the other two show up along the sharp rise of the dispersion curve of Fig. 1(b) above and below the bandgap.

From the results of $N = 1$ and 4, we can hardly imagine the band structure of $N = \infty$ shown in Fig. 1(b); the standing waves set up in a thin slab have almost nothing to do with the band structure of the ordinary band calculation. As N increases, the width of each of the DOS peaks decreases rapidly. The reason why the width decreases with increasing N is as follows: the far-field channels, responsible for the energy leakage of a WGM originally in an isolated sphere, are partly used in the lattice of spheres to lead to the hopping motions of WGM. The thicker the slab is, the less becomes the fraction of the channels that cause energy leakage.

The Q value of a slab mode is estimated by the center frequency ω_0 of the DOS peak divided by its full width at half maximum (FWHM), $\Delta\omega$. For $N = 1$, Fig. 2(a) shows that $\omega_0 \sim 50$ GHz and $\Delta\omega \sim 0.5$ GHz, and hence $Q \sim 100$ for the DOS peak of Fig. 2(a). Incidentally, the peak height measured according to the vertical axis of Fig. 2 gives a rough measure of the Q value. Note that the $\Delta\omega$'s of WGM lying in the frequency range examined are generally estimated to be a few gigahertz (they belong to $l = 1 \sim 3$ and have much larger FWHM than those used ordinarily in the cavity QED). The Q value is thus enhanced by one order, once the spheres are assembled into a 2-D regular lattice [22]. We see in Fig. 2 that the highest Q value in each DOS profile enhances roughly by one order per two layer-doubling procedures.

In the cases of $N = 32$ shown in Fig. 2(d), we emphasize once again a good correspondence of the DOS profile with the band structure given by Fig. 1(b). See, e.g., the marked decrease of DOS in the position of the bandgap. Also, each of the DOS peaks on the upper edge of the bandgap, which we noted is bounded by a flat band, suffers a marked narrowing; a band of smaller bandwidth carries standing-wave modes of higher Q values. This is a kind of rule of thumb stated in Section I. However, it is to be noted that some of the peaks present

A photonic crystal of a finite thickness is a typical example of an inhomogeneous slab system. Due to the presence of the periodicity, a complication arises in the definition of the S matrix because there can be a number of transmitted and reflected waves, specified by 2-D reciprocal lattice vectors $\boldsymbol{h}$. When the frequency of light is less than the threshold value of the first-order diffraction, the diffracted waves do not enter in the S matrix because it is defined using the far-field amplitudes. We confine ourselves to such a frequency range in the present paper. Then the scalar quantities T and R of (3) should be replaced by the 2×2 tensors, the number two coming from the degree two of the polarizations of the incident as well as the transmitted or reflected lights. In contrast to the homogeneous slab treated above, the S and P polarizations defined relative to the plane of incidence are mixed in general in the course of the scattering. Then the S matrix is of dimension 4×4, which yields four eigenphase shifts: two specified by the two directions of the polarizations of the incident light that diagonalizes the S matrix and two related again with the parity with respect to the mirror reflection (we are considering such a slab). The directions of the polarizations—diagonal polarizations—depend on $\boldsymbol{k}$ and ω, implying that we must diagonalize the S matrix for each $(\boldsymbol{k}, \omega)$ to find out the phase shifts. Note that in a homogeneous slab to which (5) applies, the directions of the P and S polarizations are fixed uniquely independently of $\boldsymbol{k}$ and ω. The expression of the DOS for the photonic crystal is then given by the same expression as (5), the sum over P and S in (5) now being replaced by the one over the two diagonal directions of the polarizations. Namely, it holds that

$$N_{\boldsymbol{k}}(\omega) = \sum_{\beta=1,\,2} \frac{1}{\pi} \frac{\partial}{\partial \omega} \left[\delta_{+}^{\beta}(\omega) + \delta_{-}^{\beta}(\omega)\right] \tag{6}$$

where $\beta = 1, 2$ specifies the two diagonal polarizations. (In the electronic case, the prefactor two appears in place of the sum over the index β.) Note that this expression holds only in the absence of the (far-field) diffracted waves.

In the general case of the presence of n open diffraction channels (n including the channel specified by $\boldsymbol{h} = 0$, which is always open), there are totally n transmitted and n reflected lights. The S matrix is then of the dimension $4n \times 4n$, leading to $4n$ eigenphase shifts. The DOS can be shown [23] to be expressed by the ω derivative of the sum of all them. The DOS given by (6) is the special case of $n = 1$.

III. Calculation of the DOS and Q Values of Slab Modes

Based on (6), we examine the DOS of the EM modes in a slab photonic crystal. We examine the cubic lattice of spheres (square lattice in a 2-D layer). We stack 2-D layers one by one to have a slab photonic crystal. We take the thickness direction as the y axis and choose the x and z axes parallel to the two sides of the square unit cell of the 2-D layer. Let N be the number of layers of the slab. In obtaining the scattering amplitude of light in the layer doubling calculation, we can access the cases of $N = 1, 2, \ldots, 2^k, \ldots$. For each N we calculated the complex transmission and reflection amplitudes to obtain the S matrix of dimension 4×4 and obtained its four eigenphase shifts. DOS was then obtained by differentiating numerically the sum of the phase shifts, according to (6). Hereafter we use the dimensionless units for $\boldsymbol{k}$, normalized by $2\pi/d$ and ω, by $2\pi c/d$, d being the lattice constant and c the light velocity. The dielectric constant of the spheres is taken to be 2.96^2 corresponding to the beads of Si_3N_4 of diameter 3.2 mm, used very recently to examine the dispersion relations of the 2-D photonic bands [22]. The lattice constant d is equal to the diameter of the spheres, and so a sphere touches with its nearest neighbors. The wave vector is chosen arbitrarily to be $\boldsymbol{k} = (0.1, k_y, 0.2)$.

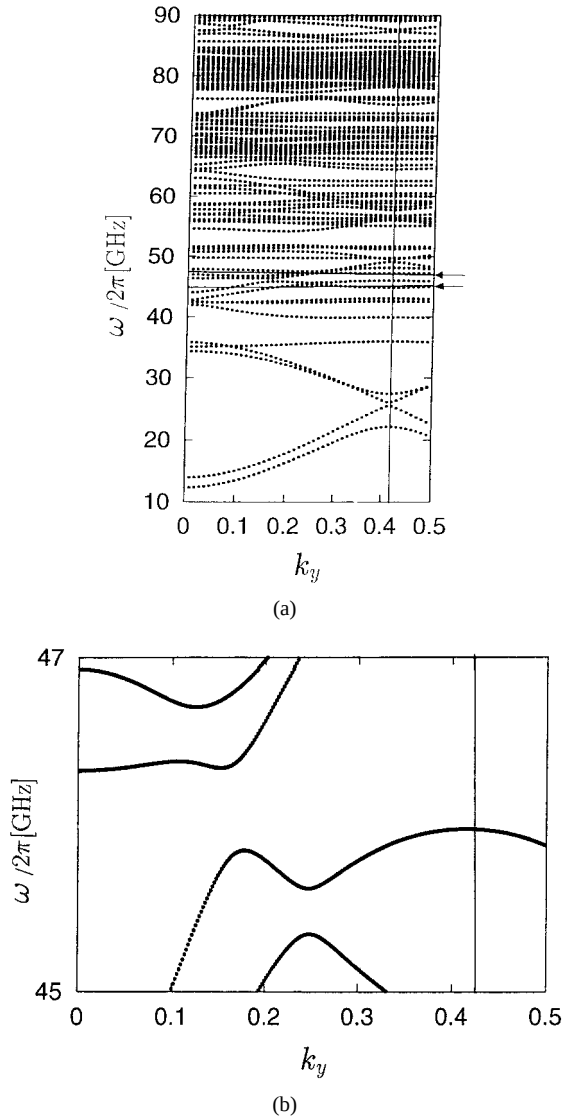

Fig. 1. Band structure of cubic lattice of dielectric spheres in units of gigahertz for $\boldsymbol{k} = (0.1, k_y, 0.2)$. (See the text for the parameters of the spheres.) A space of thickness $0.204d$ is made between the layers from an experimental reason; strictly, the lattice is tetragonal. The Brillouin-zone edge in the y direction is 0.415, which is shown by the solid line. In (b) the portion between 45 and 47 GHz is magnified.

Fig. 1(a) shows the band structure for the wave vector $(0.1, k_y, 0.2)$. We plot $\omega/2\pi$ in units of gigahertz as a function of k_y. The dimensionless frequency $\omega = 1$ is 94 GHz, which defines the frequency for the first appearance

modes is a key factor to determine the lasing; in the lasing in a photonic slab, we need an SC EM field calculated with a slab geometry taken into account honestly. Hence, a quantitatively reliable treatment of the laser action is not straightforward.

Our way adopted for this purpose is to calculate the transmittivity of light for a slab photonic lattice of active substance and to look for its divergence in the space of (ω, γ), where ω is the frequency of light and γ is the negative imaginary part of the dielectric constant. By using a negative imaginary part to simulate the population inversion, we can treat the induced emission of light in a classical way; a light-emitting atom is treated as a classical dipole moment induced by the SC field. The onset of the laser oscillation is then reduced to calculating the SC intensity of the transmitted EM field and to searching a point of its divergence in the space of (ω, γ). The narrowing of the DOS peaks with increasing thickness of the slab plays an essential role in this procedure because the sharper a peak of DOS is, the easier is the lasing associated with it or the smaller is the value of $|\gamma|$ required for the divergence to appear. For a model photonic crystal of arrayed dielectric cylinders of active substance, we are calculating the thickness dependence of the transmittivity to obtain the threshold value of γ for the onset of lasing.

We are using two model photonic crystals in this paper: an array of dielectric spheres and that of dielectric cylinders. They are both prototype photonic systems allowing a compact formulation of band calculation in terms of the vector Korringa–Kohn–Rostoker (KKR) equation. The finite thickness of a slab is taken into account in the optical response by the layer doubling method. In this method, we start from a single two-dimensional (2-D) layer and treat a slab of finite thickness by doubling the number of layers. The vector KKR formulation of the photonic band calculation is given by the author for the spheres [14]–[16] and for the cylinders [17]. The rather detailed descriptions of the layer doubling method and its application are also found there.

This paper is organized as follows. In Section II, we present the formula yielding the DOS of slab photonic crystals. Section III is devoted to applying the formula to a slab of regular array of spheres. In Section IV, we examine the onset of the lasing in an active slab of arrayed cylinders. A brief summary is given in Section V.

II. Formula for the DOS of the EM Modes in a Slab Photonic Crystal

In the scattering of an electron by a spherically symmetric potential of an atom, the increment of DOS (in this paper we often call it simply DOS by dropping "increment of") due to the presence of the scatterer, relative to that in the absence of it, is given by the famous expression familiar in the Friedel sum rule [18]

$$N(E) = \frac{2}{\pi} \sum_{l=0}^{\infty} (2l+1) \frac{\partial}{\partial E} \delta_l(E). \tag{1}$$

Here, $\delta_l(E)$ is the phase shift of the partial wave of electron of angular momentum l ($\hbar = 1$) and energy E. The factor (2l+1) incorporates the degeneracy with respect to the magnetic quantum number m. The prefactor two incorporates the spin degree of freedom. Similarly to the case of an electron, an EM field scattered by a spherical scatterer—a dielectric sphere, for example—obtains a phase shift. The degree of freedom of spin of the electronic case changes to the degree of freedom of the transverse polarization in the EM case. There are thus two vector partial-waves for each l. Unlike the potential scattering of an electron, each of the two partial-waves suffers a different scattering and obtains a different phase shift. Let us denote them by $\delta_l^{\mathrm{M}}(\omega)$ and $\delta_l^{\mathrm{N}}(\omega)$ for the partial wave of l and frequency ω, using the symbols M and N to specify the two vector partial-waves [19]. Then the DOS of the EM field per unit frequency is expressed by

$$N(\omega) = \frac{1}{\pi} \sum_{l=1}^{\infty} (2l+1) \frac{\partial}{\partial \omega} [\delta_l^{\mathrm{M}}(\omega) + \delta_l^{\mathrm{N}}(\omega)]. \tag{2}$$

The prefactor two of (1) is replaced by the presence of the two terms in the square bracket. Note that the index l runs over $l \geq 1$, reflecting the absence of the monopolar space $l = 0$ in the EM case. The scattering of a plane-wave light that corresponds to this form of DOS is just the Mie scattering. The scattered amplitude has a series of resonances due to the excitation of WGM. The lifetime of a WGM is estimated from the breadth of the ω-derivative of $\delta_l^{\mathrm{M}}(\omega)$ or $\delta_l^{\mathrm{N}}(\omega)$, which gives rise to a finite width of the corresponding Lorentzian peak in the Mie scattering.

We now turn to the scattering from a slab system [20], [21]. The phase shift of an incident wave is still a useful concept, which is introduced by using the complex amplitudes of the transmitted and reflected waves. Consider first a homogeneous slab bounded by two parallel surfaces. In this case, the transmission and reflection amplitudes are expressed by scalar quantities. Let them be T and R. In the EM scattering, both of them depend on the polarization, P or S, of the incident light. The spin degree of freedom of the electronic case is again replaced by that of the polarization in the EM scattering. In terms of T and R, the S matrix is defined by

$$\boldsymbol{S} = \begin{pmatrix} T & R \\ R & T \end{pmatrix} \tag{3}$$

which depends on the polarization of light. The amplitudes T and R appear twice in the definition because we are considering two incident waves, propagating symmetrically from above and below the slab, for the purpose of forming the standing-wave normal modes. For detail, see the recent work of the author and collaborators [22]. Since $\boldsymbol{S}$ is unitary, its eigenvalues are expressed as $\exp[2i\delta_{\boldsymbol{k}}(\omega)]$, the 2-D vector $\boldsymbol{k}$ specifying the two lateral components, parallel to the slab surface, of the incident wave vector. In this way, we can introduce two phase shifts. The two eigenphase shifts $\delta_{\boldsymbol{k}}(\omega)$ are classified by the parity of the mirror reflection with respect to the halfway of the slab. When we denote the parities by the symbols $+$ and $-$, the DOS of an electron per unit energy range due to the presence of the slab is given by

$$N_{\boldsymbol{k}}(E) = \frac{2}{\pi} \frac{\partial}{\partial E} [\delta_+(E) + \delta_-(E)] \tag{4}$$

the factor two being due to spin. In the EM case, it can be shown that the DOS per unit frequency range is given by

$$N_{\boldsymbol{k}}(\omega) = \sum_{\beta=\mathrm{P},\mathrm{S}} \frac{1}{\pi} \frac{\partial}{\partial \omega} [\delta_+^{\beta}(\omega) + \delta_-^{\beta}(\omega)]. \tag{5}$$

Density of States of Slab Photonic Crystals and the Laser Oscillation in Photonic Crystals

Kazuo Ohtaka

***Abstract*—A treatment of the density of states of electromagnetic normal modes of slab photonic crystals is given to illustrate the thickness dependence of the Q values of the slab modes of arrayed dielectric spheres. The onset of the laser oscillation is then examined for a slab photonic crystal of arrayed cylinders by simulating active cylinders as having a complex dielectric constant of negative imaginary part γ. It is shown that the divergence of the transmittivity of light occurs as an indication of the onset of lasing, when the slab is thick enough to give high Q values to the slab modes. The threshold value of γ is discussed in comparison with a one-dimensional (1-D) multilayer stack of thin films.**

***Index Terms*—Array of cylinders, array of spheres, density of states, laser action, Q value.**

I. Introduction

JUST AS in a slab ionic crystal, the lifetime of an electromagnetic (EM) mode in a slab photonic crystal depends on the slab thickness. A reliable way of estimating its magnitudes is to calculate the increment of the EM density of states (DOS) due to the presence of that mode and to examine the breadth of its peak in the DOS profile.

A rough estimate of the breadth of a DOS peak is possible if we know the total bandwidth of the photonic band, on which the peak arises, and the number of the interference fringes of the light transmission occurring on it. This estimate stems from the observation that the total bandwidth divided by the number of interference fringes over the entire dispersion curve gives the average frequency width occupied by one standing-wave solution. This crude estimate indeed works fairly well on the first band, the lowest in frequency of all photonic bands, whose dispersion curve is linear as that of a photon in free space, except for a very limited region near the band edge [1]–[3].

However, a strong scattering of EM waves characterizes photonic crystals, which induces a crossing or anticrossing among the dispersion curves and gives rise to the nontrivial band structure. As is well-known, the dispersion curves except that of the first band are far from linear, and the slab photonic modes lying on them are modified accordingly. The treatment of such slab modes is not straightforward, and the above rule of estimating the lifetime has only a qualitative meaning as a rule of thumb. Also, the EM confinement to the interior region of the slab is not complete in general and varies from mode to mode; an average frequency width is often meaningless. Furthermore, in the case of a very thin slab, the band scheme obtained for an infinite photonic crystal is no longer applicable, and the above rule of thumb loses its meaning even qualitatively. This last feature is in striking contrast to the traditional lasers, in which the propagation of light in a laser is well represented by a simple plane wave, however small the length of the active region may be.

For a quantitative understanding of a slab photonic crystal, therefore, we have to have a way of calculating the DOS of its EM normal modes. Since the actual use of photonic crystals is made on a slab system, the concept of DOS of a system of finite thickness is very important. Just as the Q value of whispering gallery modes (WGM) of a single sphere in the cavity quantum electrodynamics (QED), the Q value of the EM modes of a slab photonic crystal, inversely proportional to the breadth of the DOS peak, will play a key role in determining the various optical properties of photonic crystals, the laser action in active photonic crystals, for example.

The first purpose of this paper is to present a way of calculating the EM DOS of a slab photonic crystal from the data of transmission and reflection of light. For a model photonic slab of arrayed spheres, we show how the method works and how the resulting Q values of slab modes vary with the slab thickness. Besides the magnitudes of the Q values, or the lifetimes, of the EM slab modes, we wish in the present paper to know whether or not a peak of DOS has a precise correspondence to a peak of the transmission coefficient (dip of the reflectivity). This information will be important when we are to extract the properties of photonic bands from the experimental optical data.

The second purpose of this paper concerns the laser action in a photonic crystal. As a number of authors showed, the EM intensity is strikingly enhanced when the incident light excites an EM state at the portion of large band bending of a photonic band [4]–[8]. This means that an enhancement of the induced-emission rate and hence the laser action will be induced there most easily [9], [10]. Indeed several groups have already observed the laser oscillation in photonic crystals [11]–[13]. We believe that their observation is more or less related to the band edge effect of photonic bands.

As in traditional lasers, the onset of lasing in an active photonic crystal will be determined by the balance between the loss and gain of the EM field in a round trip of propagation. To analyze the onset of the lasing quantitatively, we need a reliable treatment of both the loss and gain, both determined by the self-consistent (SC) form of the EM field set up in a slab photonic crystal. It is then obvious that the Q value of slab

Manuscript received April 6, 1999; revised August 13, 1999. This work was supported by the Ministry of Education, Science, Sports and Culture of Japan under Grant-in-Aid for Scientific Research on Priority Area and by Science Promotion, Casio Co., Ltd.

The author is with the Center for Frontier Science, Chiba University, Inage-ku, Chiba-shi 263-8522 Japan (e-mail: ohtaka@j90.tg.chiba-u.ac.jp).

Publisher Item Identifier S 0733-8724(99)08815-5.

0733–8724/99$10.00 © 1999 IEEE